Engineering recombinant reoviruses with tandem repeats and a tetravirus 2A-like element for exogenous polypeptide expression

Aleksander A. Demidenko[a,1], Joseph N. Blattman[b,2], Negin N. Blattman[b,2], Philip D. Greenberg[b], and Max L. Nibert[a,3]

[a]Department of Microbiology and Immunobiology, Harvard Medical School, Boston, MA 02115; and [b]Department of Immunology, University of Washington School of Medicine, Seattle, WA 98195

Edited by Peter Palese, Mount Sinai School of Medicine, New York, NY, and approved April 1, 2013 (received for review January 15, 2013)

We tested a strategy for engineering recombinant mammalian reoviruses (rMRVs) to express exogenous polypeptides. One important feature is that these rMRVs are designed to propagate autonomously and can therefore be tested in animals as potential vaccine vectors. The strategy has been applied so far to three of the 10 MRV genome segments: S3, M1, and L1. To engineer the modified segments, a 5′ or 3′ region of the essential, long ORF in each was duplicated, and then exogenous sequences were inserted between the repeats. The inner repeat and exogenous insert were positioned in frame with the native protein-encoding sequences but were separated from them by an in-frame "2A-like" sequence element that specifies a cotranslational "stop/continue" event releasing the exogenous polypeptide from the essential MRV protein. This design preserves a terminal region of the MRV genome segment with essential activities in RNA packaging, assortment, replication, transcription, and/or translation and alters the encoded MRV protein to a limited degree. Recovery of rMRVs with longer inserts was made more efficient by wobble-mutagenizing both the inner repeat and the exogenous insert, which possibly helped via respective reductions in homologous recombination and RNA structure. Immunogenicity of a 300-aa portion of the simian immunodeficiency virus Gag protein expressed in mice by an L1-modified rMRV was confirmed by detection of Gag-specific T-cell responses. The engineering strategy was further used for mapping the minimal 5′-terminal region essential to MRV genome segment S3.

Orthoreovirus | Reoviridae | dsRNA virus | viral vector

The goal of the work described here was to implement a strategy for engineering recombinant mammalian reoviruses (rMRVs) to serve as transduction vectors for expressing exogenous polypeptides over multiple cycles of viral growth in the absence of further technological intervention such as expression of essential viral proteins *in trans*. To date, such autonomously propagating rMRV vectors have proven difficult to generate. One reason for trying to develop such rMRVs might be to test them as potential vaccine vectors for eliciting responses to exogenous immunogens expressed in animals.

MRVs constitute one of five approved species in genus *Orthoreovirus*, family *Reoviridae* (1). Their genomes each comprise 10 linear segments of dsRNA, which are packaged inside nonenveloped, double-layered, icosahedral protein capsids in infectious virions (2–4). MRVs are widespread in mammals, including humans, but are not a regular cause of serious human disease. Nonetheless, they provide several useful models for studies of viral phenomena, including the pathogenesis of virally induced diseases in laboratory animals (5, 6). They are also a source of interest as oncolytic agents, with possible use in treating human cancers (7).

Approaches for obtaining MRV mutants by screening or forward selection have been developed and fruitfully applied for many years (8, 9), but reverse genetics methods for MRV have been slower to develop. In the late 1990s, an approach called "recoating genetics" was reported, involving in vitro reconstitution of MRV virions with engineered, mutant forms of the outer-capsid proteins for subsequent studies of cell entry (10, 11). Beginning even earlier and continuing toward the present, a system for incorporating plasmid-transcribed RNA into infectious viruses was also reported and has been used for mapping essential terminal regions of some of the MRV genome segments (12–14). Then, in 2007, a simpler and more versatile system for recovering infectious rMRVs from cotransfected plasmid constructs of all 10 genome segments was reported (15), allowing reverse genetics on a much broader scale (16–19).

In addition to use for reverse genetics, the plasmid-based systems have given promise to the notion of developing rMRVs as expression vectors for exogenous polypeptides. In studies with each of the plasmid-based approaches, results have shown that rMRVs can express a reporter protein (chloramphenicol transferase or green fluorescent protein) during infection (12, 15). The limitation of those results has been that the approach involves expressing one of the essential MRV proteins *in trans*, as the genome segment normally encoding that protein has been modified to encode the reporter instead. As a result, multiplication of these reporter-expressing rMRVs occurs only in cells expressing the missing MRV protein *in trans*. More recently, two groups have reported success at generating rMRVs with exogenous sequences encoding up to 40 aa fused to the C terminus of MRV protein σ1, encoded by segment S1, without the need for *trans* expression of native σ1 (20, 21). Despite these advances, a strategy for gener-

Significance

Recombinant reoviruses that can propagate autonomously while expressing exogenous polypeptides over multiple growth cycles have proven difficult to generate but seem plausible to try to develop as potential vaccine vectors. Here we report a strategy for engineering such reoviruses that express portions of the simian immunodeficiency virus Gag protein. The strategy has been applied so far to 3 of the 10 reovirus genome segments and can also be used to map the terminal regions required for segment packaging. Gag-specific T-cell responses induced in mice by one of these recombinant reoviruses support their potential utility as vectors for immunogen expression.

Author contributions: A.A.D., J.N.B., N.N.B., P.D.G., and M.L.N. designed research; A.A.D., J.N.B., and N.N.B. performed research; A.A.D. contributed new reagents/analytic tools; A.A.D., J.N.B., N.N.B., P.D.G., and M.L.N. analyzed data; and A.A.D., J.N.B., N.N.B., P.D.G., and M.L.N. wrote the paper.

The authors declare no conflict of interest.

This article is a PNAS Direct Submission.

[1]Present address: Department of Microbiology, The Forsyth Institute, Cambridge, MA 02142.

[2]Present address: School of Life Sciences, Infectious Diseases, and Vaccinology, Arizona State University, Tempe, AZ 85287.

[3]To whom correspondence should be addressed. E-mail: mnibert@hms.harvard.edu.

This article contains supporting information online at www.pnas.org/lookup/suppl/doi:10.1073/pnas.1220107110/-/DCSupplemental.

ating such autonomously propagating rMRV vectors with longer exogenous inserts in any of the 10 genome segments has yet to be reported.

In this study, we tested a strategy for engineering autonomously propagating rMRVs to serve as expression vectors for exogenous polypeptides. Results show progress toward this goal, including application to three of the 10 MRV genome segments. Immunization of mice with rMRV expressing a 300-aa portion of the simian immunodeficiency virus (SIV) strain mac239 Gag protein yielded significant Gag-specific CD8 T-cell responses, confirming in vivo expression of this exogenous polypeptide. The engineering strategy was further used for mapping the minimal 5′-terminal region essential to MRV genome segment S3.

Results

Strategy Part 1: Duplicating MRV Segment Termini to Separate ORF and PARTT Sequences. To generate autonomously propagating rMRVs that express exogenous polypeptides, we expected to need to retain all 10 genome segments because one long ORF on the plus strand of each is essential for MRV multiplication (2, 15). We also expected that propagation-competent rMRVs would need to have exogenous sequences inserted only at certain well-chosen positions within each segment, so as not to disrupt either the essential ORF or other *cis*- or *trans*-acting RNA sequences that provide essential signals for RNA packaging, assortment, replication, transcription and/or translation (PARTT). Such PARTT signals for which findings are available to date reside at both segment termini but are not restricted to the short 5′ and 3′ untranslated regions (UTRs), instead overlapping the essential ORF by perhaps >100 nt in some cases (12–14, 22, 23), as schematized in Fig. 1*A* for the MRV S3, M1, and L1 plus strands. Because the minus strand of each segment never exits the capsid during MRV replication (2), it is not a direct concern for designing rMRV vectors: Only the plus strand is transcribed and translated, and therefore our design considerations concerned only the plus strand sequences.

Because of worries about disrupting PARTT signals at the MRV segment termini, we decided to modify each targeted segment so that at one end, the ORF and PARTT sequences would be separated. To this end, we generated in-frame tandem duplications of either a 3′-terminal region of ORF sequences, ending with the stop codon (Fig. 1*B*, *Upper*), or a 5′-terminal region of ORF sequences, beginning with the start codon (Fig. 1*B*, *Lower*). In either case, we expected this duplication to need to be ∼100 nt long or more, as suggested by previous findings noted earlier regarding the length of MRV PARTT signals examined to date (12–14, 22, 23). The 5′ and 3′ duplications that we successfully used to recover rMRVs in the experiments that follow all range between 45 and 207 nt.

For expressing the essential MRV protein from such modified segments, the 3′ ORF-region duplication was expected to have no effect, as it reconstitutes the native ORF, including its stop codon (Fig. 1*B*, *Upper*). The 5′ duplication, however, leaves intact the original translational start site of the MRV protein, so that the encoded, N-terminal region of the MRV protein also was expected to be translated as a tandem duplication (Fig. 1*B*, *Lower*), possibly reducing the functionality of this essential protein. Although this represents a likely flaw, the problem was overcome by the additional element described next.

Strategy Part 2: Expressing Exogenous Polypeptide Separate from the Essential MRV Protein. Theoretically, inserted exogenous polypeptide sequences might or might not be expressed in fusion with the MRV protein. The latter option seems commonly preferable, as modifying the essential MRV protein by fusion with another polypeptide might impair or even inactivate it. We therefore sought to develop a strategy that allows an exogenous polypeptide to be expressed separately from the essential MRV protein encoded on the same, modified segment.

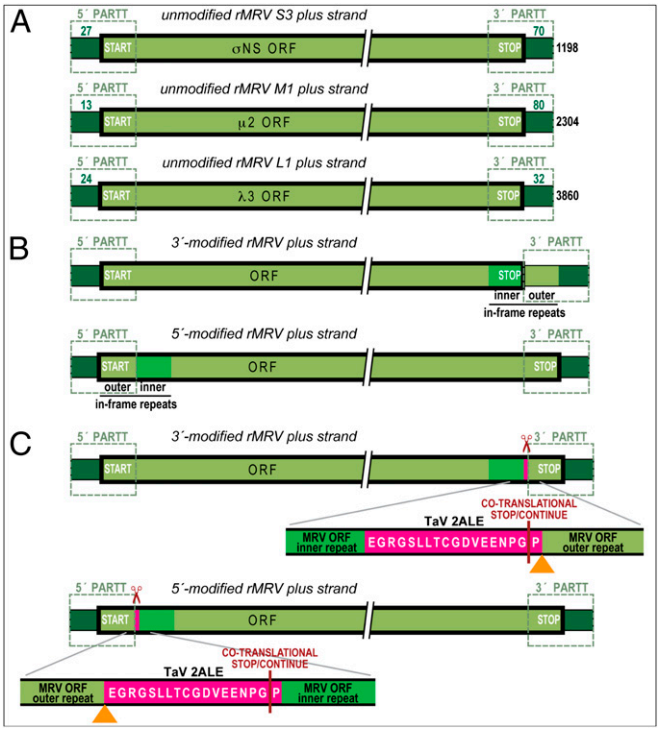

Fig. 1. Schematics of native MRV plus-strand RNAs and in-frame modifications central to the described vector strategy. The plus strands are all shown 5′ left to 3′ right and are not drawn to scale. The native 5′ and 3′ UTRs are shaded dark green, and the native ORF region is shaded light green. The ORF region is also surrounded by a thickened outline, and the start and stop codons marking the ends of the ORF are indicated. Dashed outlines indicate the 5′- and 3′-terminal regions putatively essential for PARTT. (*A*) Native S3, M1, and L1 plus strands. Lengths of the 5′ and 3′ UTRs (in nt) are shown, along with the total length at right. (*B*) In-frame, 3′ (*Upper*) and 5′ (*Lower*) ORF-region duplications in a representative MRV plus-strand RNA. The inserted, inner repeats are shaded bright green. (*C*) In-frame insertion of the TaV 2ALE in a representative MRV plus-strand RNA. The position of the inserted 2ALE (magenta) is shown in the setting of the in-frame 3′ (*Upper*) and 5′ (*Lower*) ORF region duplications. Scissors indicate the 2ALE-specified, cotranslational stop/continue event. The aa sequence of the 2ALE is shown in the lower inset of each schematic, along with parts of the flanking MRV inner and outer repeats. A vertical bar in each inset indicates the position of the cotranslational stop/continue event. Orange arrowheads indicate where additional sequences for exogenous polypeptide expression will be later inserted.

Our specific strategy made use of a "2A-like" element (2ALE) that mediates a cotranslational stop/continue event, which has been naturally exploited by picornaviruses, tetraviruses, and others as an apparently nonproteolytic means for polyprotein processing (24, 25). In particular, we used the 2ALE from betatetravirus Thosea asigna virus (TaV) (26), which has the nucleotide sequence GAGGGCAGGGGCAGCCTGCTGACCTGCGGCGACGTGGAGGAGAACCCCGGCCCC (encoding EGRGSLLTCGDVEENPGP) and was chosen for being one of the smallest of these elements known (54 nt encoding 18 aa in all constructs containing it below), for having one of the highest known efficiencies of stop/continue activity (>99%) (24), and for having been previously used in retrovirus vectors to good effect (27). The 2ALE is thought to function such that translation stops after the Gly residue in the penultimate C-terminal position of the element, but then continues, with the C-terminal Pro residue of the element becoming the N-terminal residue of the separate, downstream product. As a result, when inserted immediately after an MRV protein-encoding sequence, not including the stop codon, the 2ALE adds only 17 C-terminal aa (EGRGSLLTCGDVEENPG)

to the MRV protein (Fig. 1*C*, *Upper*), and when inserted immediately before, it adds only a single N-terminal Pro (Fig. 1*C*, *Lower*).

In addition, insertion of the 2ALE also salvages the 5′-duplication approach from the flaw described earlier: The cotranslational stop/continue event is expected to release not only the N-terminal 17 aa of the 2ALE but also the N-terminally duplicated region of the MRV protein that precedes the 2ALE (Fig. 1*C*, *Lower*). The downstream, intact MRV protein should then go on to be translated with only the single new 2ALE-encoded Pro residue at its N terminus.

Duplicating the 5′- or 3′-Terminal ORF Region and Inserting the 2ALE. We first tested the 3′ duplication strategy. In this case, the inner repeat provides the protein coding sequences and is translated as part of the full-length MRV protein, whereas the outer repeat, together with the 3′ UTR, is expected to provide the PARTT signals (Fig. 1*B*, *Upper*). In this manner, we succeeded in recovering and passaging rMRV isolates with a duplication of the last 153 nt (51 codons including the stop) of the μ2-encoding ORF of segment M1 (Fig. 2*A*, *Upper*), as confirmed by RT-PCR-based sequencing of RNA extracted from the passaged stocks (passage level three for this and all other rMRVs described later; *Materials and Methods*) and as reflected by slower gel migration of the M1 dsRNA (Fig. 2*B*). This rMRV, designated M1/3′153 (M1 segment has a 3′ ORF-region repeat of 153 nt) forms similar to slightly larger plaques relative to rMRV containing all 10 wild-type (WT) segments (*Materials and Methods*) (15).

On the basis of the preceding considerations, one notable feature of M1/3′r153 is that it does not contain a 2ALE, and thus does not encode a C-terminal fusion to MRV μ2. We therefore next attempted to incorporate the TaV 2ALE into this virus immediately downstream of the μ2 ORF. Previous work has shown that μ2, when expressed from a plasmid *in trans*, can tolerate a C-terminal fusion and remain functional for complementation (28), which is why we targeted it for this first attempt at adding the 17-aa C-terminal fusion from the 2ALE. The resulting rMRV, M1/3′153/2A (Fig. 2*A*, *Middle*), was recovered, passaged, sequence-confirmed from the passaged stocks, and showed similar growth characteristics to rMRV WT, as suggested by a single-cycle growth-curve experiment (Fig. 2*C*).

We next tested the 5′ duplication strategy. In this case, the outer repeat, together with the 5′ UTR, is expected to provide the PARTT signals, whereas the inner repeat provides the protein coding sequences and is translated as part of the full-length MRV protein. In fact, this 5′ approach, after addition of the 2ALE, seems more advantageous than the 3′ one: As discussed earlier, in the 5′ approach, the 2ALE adds only a single N-terminal Pro to the essential MRV protein, whereas in the 3′ approach, the 2ALE adds 17 C-terminal residues, increasing chances that the MRV protein will be impaired. Using the 5′ approach, we succeeded in recovering and passaging several different rMRVs, as described in more detail later, including 2ALE fusions to the *N* termini of MRV protein σNS encoded by segment S3 (Fig. 2), MRV protein μ2 encoded by segment M1 (Table 1), and MRV protein λ3 encoded by segment L1 (Fig. 3). Most pertinent to the progression of descriptions here, in rMRV S3/2A/5′174 (S3 segment has a 5′ ORF-region repeat of 174 nt, with an in-frame 2ALE preceding the inner copy of the repeat; Fig. 2*A*, *Lower*), the presence of these modifications to S3 was confirmed by sequencing from the passaged stocks and was reflected by slower gel migration of the S3 dsRNA (Fig. 2*D*).

The described strategy for expressing exogenous polypeptides apart from the MRV proteins requires proper functioning of the 2ALE. However, in the case of the 5′ approach, there seems to be a chance that translation of the MRV protein might involve an internal initiation mechanism that bypasses the 2ALE and begins translation at or near the MRV start codon retained at the 5′ end of the inner repeat. To address this possibility, we introduced a 1-nt deletion (Δ1) into the middle of the 2ALE in construct (plasmid, p) pS3/2AΔ1/5′174, causing a −1 translational frameshift that eliminates not only 2ALE function but also in-frame translation of σNS. Alternatively, if synthesis of σNS occurs via an internal translation-initiation mechanism, the 1-nt deletion in the 2ALE should have little or no effect. Using RNA transcribed from the plasmid constructs in in vitro translation reactions, we found that pS3/WT (15) (Fig. 1*A*, *Upper*) and pS3/2A/5′174 (Fig. 2*A*,

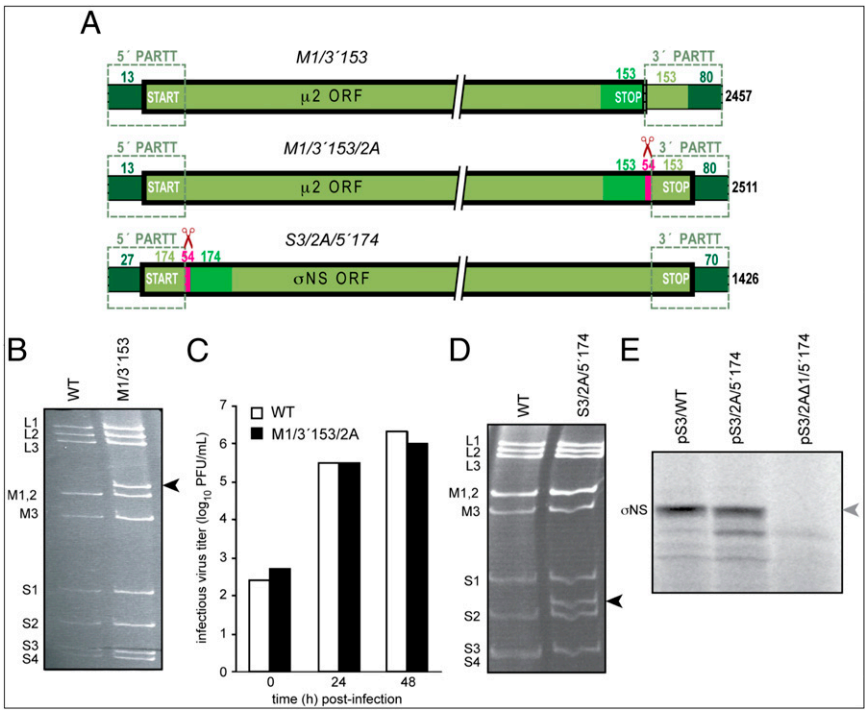

Fig. 2. rMRVs with in-frame 5′ or 3′ ORF region duplication, with or without in-frame 2ALE insertion. (*A*) Schematics of the modified M1 or S3 plus-strand RNAs used for creating these rMRVs. See Fig. 1 for labeling and color schemes. The in-frame outer repeat, inner repeat, and 2ALE lengths (in nt) are now also labeled in each schematic. (*B*) Electropherogram of genomic dsRNAs from native MRV-T3D (purified virions) and rMRV M1/3′153. The band corresponding to the slower-migrating, lengthened M1 segment of M1/3′153 is indicated (arrowhead). (*C*) Parallel growth in L929 cells by rMRVs WT (white bars) and M1/3′153/2A (black bars). (*D*) Electropherogram of genomic dsRNAs from rMRVs WT and S3/2A/5′174. The band corresponding to the more slower-migrating, lengthened S3 segment of S3/2A/5′174 is indicated (arrowhead). (*E*) Fluorogram of [^{35}S]Met-labeled in vitro translation products of plus-strand RNAs transcribed from the indicated plasmid constructs of MRV segments. Constructs pS3/2A/5′174 and pS3/2AΔ1/5′174 are identical except for a 1-nt deletion in the latter, which inactivates the 2ALE and places the downstream σNS ORF out of frame with the 2ALE and upstream sequences. The lack of a full-length σNS band translated from pS3/2AΔ1/5′174 RNA is indicated (gray arrowhead).

Table 1. Introducing SIVmac239 *gag* inserts for recovery into rMRVs

Modified MRV segment*	*gag*-insert length in nt (codons)	rMRV recovery?†
S3/*gag*##/2A/5′69w	27 (9)	YES
	57 (19)	YES
	87 (29)	NO
	117 (39)	NO
	177 (59)	NO
S3/*gag*##CM9/2A/5′69w	27 (9)	YES
	57 (19)	YES
	87 (29)	NO
	117 (39)	NO
M1/*gag*##/2A/5′195w	27 (9)	YES
	57 (19)	YES
	117 (39)	YES
	147 (49)	NO
L1/*gag*##/2A/5′66w	27 (9)	YES
	57 (19)	YES
	117 (39)	YES
	147 (49)	NO
	177 (59)	NO
	237 (79)	NO
	297 (99)	NO
L1/*gag*##/2A/5′207w/3′168	27 (9)	YES
	57 (19)	YES
	117 (39)	YES
	177 (59)	NO

*Nomenclature is as follows: modified segment/*gag* insert length/54-nt 2ALE/plus-strand terminus or termini at which duplication(s) made and length of the inner repeat (w, wobble mutagenized). The number signs (##) indicate different *gag*-insert lengths in nt as listed in the second column. The *gag* inserts all extend from the sequences for murine T-cell epitope KV9, except for the *gag* inserts in S3/*gag*##CM9/2A/5′69w, which extend from the sequences for primate T-cell epitope CM9.

†Construct pL1/*gag*##/2A/5′207w/3′168 was cotransfected with pM1/3′153 to recover virus in these experiments.

Lower) yielded primary translation products that comigrated near the expected position of σNS (41 kDa) by SDS/PAGE (Fig. 2*E*). The 1-nt deletion in pS3/2AΔ1/5′174, in contrast, eliminated synthesis of this expected protein (Fig. 2*E*). Together these findings suggest that synthesis of full-length σNS from pS3/2A/5′174 involves translation initiation upstream of the 1-nt deletion in the 2ALE, and therefore relies on proper 2ALE function to yield 41-kDa σNS (actually Pro-σNS). In addition, in accordance with this lack of σNS expression from pS3/2AΔ1/5′174 in vitro, no rMRV plaques were obtained from plasmid cotransfections of L929 cells, including this construct in place of pS3/WT.

Wobble-Mutagenizing the Inner Repeat. Having succeeded in generating rMRV S3/2A/5′174, we moved on to try to insert additional exogenous sequences in the S3 segment. We first inserted 150 nt (50 codons) from the *gag* gene of SIVmac239 (GenBank accession no. M33262) (29) (Fig. S1*A*) immediately upstream of and in frame with the TaV 2ALE in pS3/2A/5′174, yielding the construct pS3/*gag*150/2A/5′174 (Fig. S1*B*). When used to recover the respective rMRV, we recovered viral plaques, although at only ∼10% of the usual efficiency relative to other successful constructs in this report. Moreover, on sequencing of the S3 segment from passaged stocks of several of these isolates, we found WT S3 in all of them, as also suggested by the WT-like gel migration of the S3 dsRNA (Fig. S1*C*).

To troubleshoot why only WT S3 had been recovered in these isolates, we repeated the experiment, substituting the previously described construct pM1/3′153 (Fig. 2*A*) for pM1/WT (15). Thus, in this experiment, constructs for two modified segments, S3 and M1, were used for recovering rMRV. Viral plaques were again recovered, although again at reduced efficiency, and when analyzed by electrophoresis of viral dsRNA and sequencing from passaged stocks, all of the recovered isolates were found to contain the modified M1 segment and, again, the WT S3 segment (Fig. S1*C*). Having recovered WT S3 after transfection of pS3/*gag*150/2A/5′174 in two separate experiments, with care to avoid contamination, we concluded that either homologous recombination or template skipping between the 5′ repeats was the likely cause of restoring WT S3 in these rMRVs.

One method to overcome homologous recombination between repeats is to introduce numerous differences between them. To achieve this, we exhaustively mutagenized the wobble positions of the inner, protein-coding repeat of the 5′-modified constructs (Fig. S2*A*). In this strategy, the outer repeat, which is expected to provide the PARTT signals, remains unchanged, whereas the inner repeat is changed in its RNA sequences but not its encoded protein sequences. As illustrated in Fig. S2*B* for a wobble-mutagenized L1 segment, this procedure can reduce RNA sequence identity to <60% between the two repeats. This approach has proven successful, in that we have observed no examples of reversions to WT sequences in the modified segments of any subsequently recovered rMRVs described later. As a result, we consider recombination, not skipping, to have been the more likely cause of the original problem.

Inserting Progressively Longer *gag* Inserts. Having solved the apparent problem of recombination between the repeats, we returned to trying to insert additional exogenous sequences in the S3 segment, this time using base construct pS3/2A/5′69w, in which the inner, 69-nt repeat of 5′ ORF sequences was wobble-mutagenized (w). We began by inserting only 9 codons (27 nt) from the SIVmac239 *gag* gene immediately upstream of and in frame with the TaV 2ALE, and in this case, the encoded 9 aa represented the murine T-cell epitope KV9 from Gag region p17 (30) (construct pS3/*gag*27/2A/5′69w). The resulting rMRV was indeed recovered, passaged, and sequence-confirmed from the passaged stocks (Table 1). We next increased the length of the *gag* insert by including codons immediately downstream of the KV9-encoding sequences. The construct containing 19 *gag* codons (57 nt; construct pS3/*gag*57/2A/5′69w) also yielded rMRV plaques that were passaged and sequence-confirmed from the passaged stocks; however, longer *gag* inserts containing 29, 39, or 59 codons (87, 117, or 177 nt) did not yield plaques from the plasmid cotransfections (Table 1).

One idea for why we had failed to recover longer *gag* inserts in rMRVs was that the specific Gag sequences beyond the first 19 aa in the preceding experiment might have been toxic. To test this idea, we replaced the original *gag* sequences with ones encoding part of SIVmac239 Gag region p24; specifically, ones containing the primate T-cell epitope CM9 (31) plus 0, 10, 20, 30, or 50 downstream codons. Identical results were obtained as with the respective KV9-encoding constructs (Table 1), leading us to conclude that toxicity was an unlikely explanation for failing to recover the longer *gag* inserts in rMRVs.

Another idea was that the smallness of segment S3 might somehow limit the size of inserts that can be tolerated, and perhaps one of the larger MRV genome segments could tolerate longer ones. To test this possibility, we used L1, encoding protein λ3, and M1, encoding protein μ2. In line with our strategy, justified by findings presented earlier, L1 was modified to contain a wobble-mutagenized inner repeat of the 5′ ORF region (66 nt; 22 aa of λ3), preceded by a TaV 2ALE insertion, preceded by an SIVmac239 *gag* insert encoding the 9-aa KV9 epitope plus increasing numbers of downstream codons in different constructs (base construct pL1/*gag*27/2A/5′66w). M1 was comparably modified, except the wobble-mutagenized inner repeat of its 5′ ORF region was longer (195 nt; 65 aa of μ2; base construct pM1/*gag*27/2A/5′195w). With L1 and M1 each modified in these ways, the

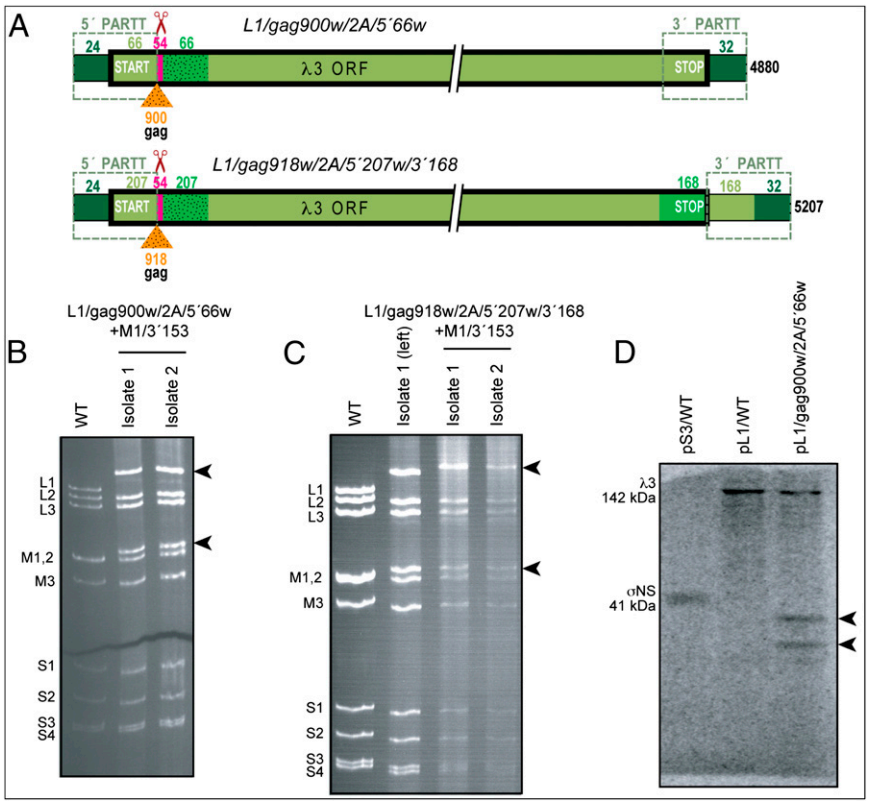

Fig. 3. rMRVs with long SIVmac239-*gag* inserts. (*A*) Schematics of the in-frame-modified L1 plus-strand RNAs used for creating these rMRVs. See Figs. 1 and 2 for labeling and color schemes. (*B* and *C*) Electropherograms of genomic dsRNAs from rMRVs WT (purified virions) and two separately plaque-derived isolates of L1/*gag*900w/2A/5′66w+M1/3′153 (*B*) and L1/ *gag*918w/2A/5′207w/3′168+M1/3′153 (*C*). Note that for recovering these rMRVs, both modified L1 and modified M1 constructs were used, and the two dsRNA bands corresponding to these slower-migrating, lengthened segments are indicated in both *B* and *C* (arrowheads). For *C*, isolate 1 from *B* was rerun for comparison; the L1 segment in rMRV L1/*gag*918w/2A/5′207w/3′168+M1/3′153 is 327 bp longer than the one in L1/*gag*900w/2A/5′66w+M1/3′153, which explains its even slower migration. (*D*) Fluorogram of [^{35}S]Met-labeled, in vitro translation products of plus-strand RNAs transcribed from the indicated plasmid constructs of MRV segments. Construct pL1/*gag*900w/2A/5′66w RNA yields two bands consistent with the expected Gag-containing polypeptide and a putative breakdown product (arrowheads).

longest *gag* insert for which rMRV plaques were recovered, passaged, and sequence-confirmed from the passaged stocks was 39 codons (117 nt) (Table 1). The constructs containing longer *gag* inserts did not yield plaques from the plasmid cotransfections. Thus, although the insert length achieved in M1 and L1 was about twice that achieved in S3, the smaller size of S3 seems unlikely to be the main determining factor of the observed limitation to recovering rMRVs with even longer *gag* inserts.

However, another idea was that a volume- and function-defined restriction on how much dsRNA can be packaged inside the MRV capsid (*Discussion*), regardless of which segment is involved, might limit the size of inserts that can be tolerated. The intracapsid concentration of MRV genomic dsRNA normally approximates 400 mg/mL (32), so that progressive insertion of longer exogenous sequences within any of the segments would increase this already high concentration and might quickly affect virus viability.

To explore this possibility, we modified the L1 segment to contain a longer, wobble-mutagenized, 5′ ORF-region duplication (207 nt [Fig. S2*B*] vs. 66 nt in the previous construct), in addition to a 3′ ORF-region duplication of 165 nt. The resulting base construct, pL1/*gag*27/2A/5′207w/3′168, was thus 306 nt longer than the previous base construct, pL1/*gag*27/2A/5′66w. Moreover, to increase the genome size even further, we used the pM1/3′153 construct in place of pM1/WT. With these modified L1 and M1 segments, the longest SIVmac239 *gag* insert for which rMRV plaques were recovered, passaged, and sequence-confirmed from the passaged stocks was again only 39 codons (117 nt) (Table 1). Thus, as the addition of 306 + 153 = 459 nt in the inner repeats of the L1 and M1 segments did not affect the lengths of *gag* inserts that could be recovered in rMRVs, the restriction on how much more dsRNA can be tolerated inside the MRV capsid is also unlikely to be the main determining factor of the observed limitation to *gag*-insert length over the tested range of insert sizes, although it is still expected to be a determining factor for even longer inserts (*Discussion*).

Reducing RNA Secondary Structure in the *gag* Inserts. Despite our preceding efforts, we retained the problem of how to recover rMRVs with SIVmac239 *gag* inserts longer than 19 codons in S3 or 39 codons in M1 or L1. We therefore next considered that the longer *gag* inserts might be forming more stable RNA structures, which might in turn limit the capacity of the inserted sequences to be packaged, assorted, replicated, transcribed, and/or translated when part of an MRV plus strand. In Fig. S2*D Left*, for example, we show the predicted RNA secondary structure of the 50-codon *gag* insert following the KV9-encoding sequences in constructs pS3/ *gag*177/2A/5′69w, and so on, that were tested for rMRV recovery, as shown in Table 1. This predicted structure has a calculated minimum free energy of −49.7 kcal/mol. To test whether reducing this structure propensity might improve its recovery in rMRVs, we extensively wobble-mutagenized the 50-codon portion of the insert in a manner intended to reduce its predicted structure while preserving its encoded protein sequence. In Fig. S2*D Right*, we show the predicted RNA secondary structure of this wobble-mutagenized insert, which now has a calculated minimum free energy of only −16.4 kcal/mol. This and other wobble-mutagenized inserts also have lower G+C contents consistent with their reduced structure-forming propensities.

The wobble-mutagenized, 50-codon *gag* insert was indeed recovered in rMRV plaques, passaged, and sequence-confirmed from the passaged stocks of not only L1/*gag*177w/2A/5′66w but also L1/*gag*177w/2A/5′207w/3′168 (Table 2). Furthermore, even much longer wobble-mutagenized *gag* inserts were also recovered in rMRV plaques, passaged, and sequence-confirmed from the passaged stocks, as indicated in Table 2. As expected, the longest of these wobble-mutagenized inserts tested to date, 300–306 codons (900–918 nt) in constructs pL1/*gag*900w/2A/5′66w (Fig. 3*A*, *Upper*) and pL1/*gag*918w/ 2A/5′207w/3′168 (Fig. 3*A*, *Lower*), exhibit markedly slower gel migration of the L1 dsRNA in their respective rMRVs (Fig. 3 *B* and *C*). Wobble-mutagenizing the exogenous insert to reduce predicted RNA

Table 2. Introducing wobble-mutagenized SIVmac239 *gag* inserts for recovery into rMRVs

Modified MRV segment*	*gag*-insert length in nt (codons)	rMRV recovery?†
L1/*gag*##w/2A/5′66w	27 (9)	YES
	57 (19)	YES
	117 (39)	YES
	177 (59)	YES
	357 (119)‡	YES
	597 (199)‡	YES
	900 (300)‡,§	YES
L1/*gag*##w/2A/5′207w/3′168	27 (9)	YES
	57 (19)	YES
	117 (39)	YES
	177 (59)	YES
	357 (119)‡	YES
	597 (199)‡	YES
	918 (306)‡,§,¶	YES

*Nomenclature is defined in Table 1. Number signs (##) indicate the different *gag*-insert lengths in nt, as listed in the second column. These wobble-mutagenized (w) *gag* inserts all extend from the sequences for murine T-cell epitope KV9.

†Both constructs were cotransfected and recovered with pM1/3′153 in these experiments. The same experiment done for pL1/*gag*##w/2A/5′66w with pM1/WT gave the same results.

‡These inserts also encompass the sequences for primate T-cell epitope CM9.

§These inserts also encompass the sequences for murine T-cell epitope AL11.

¶This insert encodes 300 codons of *gag* plus 6 His codons.

structure thus seems to represent a useful strategy element for increasing insert size into a range at which many full-length proteins (up to ∼34 kDa thus far) can be encoded.

It should be noted that for the preceding experiments in this section, we used pM1/3′153 in place of pM1/WT. We did this because rMRV M1/3′153 generally forms slightly larger plaques than rMRV WT, and we therefore thought that this 3′-modified M1 might provide a growth advantage for viruses with other modified segments that we had yet to test. The experiments with base construct pL1/*gag*27/2A/5′66w were nevertheless repeated with pM1/WT and gave identical results to those with pM1/3′153 (Table 2).

We took advantage of the new L1 constructs with much longer *gag* inserts to perform an experiment suggesting successful translation of the Gag-containing polypeptide. Using RNA transcribed in vitro from the plasmid constructs, we found that pS3/WT (Fig. 1*A*, *Upper*), pL1/WT (15) (Fig. 1*A*, *Lower*), and pL1/*gag*900w/2A/5′66w (Fig. 3*A*, *Upper*) yielded primary in vitro translation products that migrated near the expected position of either σNS (41 kDa) or λ3 (142 kDa) after SDS/PAGE (Fig. 3*D*). Furthermore, translation of RNA from pL1/*gag*900w/2A/5′66w, but not pL1/WT, yielded two other major products in the 30- to 40-kDa range (Fig. 3*D*). The calculated size of the predicted upstream polypeptide from pL1/*gag*900w/2A/5′66w, preceding the 2ALE stop/continue event, is 37.6 kDa (22 N-terminal aa of λ3 + 300 aa of Gag + 17 N-terminal aa of the 2ALE), and we therefore argue that the observed 30- to 40-kDa gel bands probably represent this Gag-containing polypeptide and a putative breakdown product.

Immunogenicity of MRV-Encoded Gag Polypeptide Expressed in Mice. To test directly whether polypeptides encoded by rMRVs could be expressed and serve as effective immunogens in vivo, we immunized mice with purified rMRV virions (*Materials and Methods*). In an initial experiment, we compared rMRVs WT, S3/2A/5′69w, and S3/*gag*27/2A/5′69w (Table 1) but observed no significant anti-Gag responses to any of these. Considering that the region of Gag expressed by S3/*gag*27/2A/5′69w is quite small, we next tested rMRV L1/gag900w/2A/ 5′66w+M1/3′153 (Fig. 3), which (as noted earlier) expresses a 300-aa portion of SIVmac239 Gag, including the previously defined KV9 and AL11 murine T-cell epitopes (30). Other mice were immunized with purified virions of rMRV WT as a negative control. To assess the relative immunogenicity of the Gag polypeptide expressed by rMRV compared with other viral vaccine platforms, we also immunized mice with purified virions of a replication-deficient recombinant adenovirus 5 vector (Ad5-Gag; E1–E3 deleted) that expresses SIVmac239 Gag and has been previously shown to induce potent T-cell responses (33). To assess background detection levels, a final group of mice was mock immunized with PBS. As expected, mock-immunized mice or mice that received rMRV WT had little or no detectable CD8 T-cell responses to either KV9 or AL11 peptide compared with no-peptide control mice (Fig. 4). However, mice immunized with rMRV L1/*gag*900w/2A/5′66w+M1/3′153 had significant CD8 T-cell responses to both peptides (Fig. 4). Even though these rMRV-induced responses were lower than those by the well-established Ad5-Gag vector, they nonetheless clearly demonstrate that the Gag polypeptide was expressed by rMRV in vivo and in a manner that led to immune recognition and response. Moreover, results obtained with different doses of the Gag-expressing rMRV (Fig. S3) suggest that even higher doses of this vector would likely provide even higher responses.

Identifying the Minimum 5′-Terminal PARTT Region of MRV Genome Segment S3. Using a 5′-modified S3 segment, we performed a distinct type of experiment to demonstrate the additional utility of the engineering strategy for analyzing the PARTT region of an MRV genome segment. Starting with base construct pS3-*gag*27/2A/5′174w, we progressively reduced the length of the 5′-terminal region preceding the insertions, as indicated in Table 3. In the base construct, this region includes the 27-nt 5′ UTR plus the 174-nt outer repeat, for a total length of 201 nt. All of the differently sized regions in Table 3 share the native S3 5′ terminus, as the length reduction in each construct was obtained by deleting sequences from the inner (3′) end of the outer repeat. Lengths of the 5′-terminal region ranging from 201 nt down to 45 nt yielded rMRV plaques that were passaged and sequence-confirmed from the passaged stocks, whereas lengths ≤42 nt or more did not yield plaques from the plasmid cotransfections (Table 3). We therefore conclude that the minimal portion of the S3 5′-PARTT region that can tolerate the *gag* and 2ALE insertions in rMRVs is only 45 nt long: the 27-nt 5′ UTR plus 18 nt of the σNS ORF. Moreover, as the inner repeat in these constructs was exhaustively wobble-mutagenized, it seems unlikely that those sequences could have continued to contribute to 5′-PARTT activities, suggesting that the entire essential 5′-PARTT signals of S3 lie within these 5′-terminal 45 nt.

Discussion

In this study, we tested a strategy for generating autonomously propagating rMRVs as transduction vectors to express exogenous polypeptides. The engineering strategy, as refined during these experiments, involves three main elements: in-frame insertion of a wobble-mutagenized copy of a 5′-terminal region of MRV ORF sequences, in-frame insertion of the TaV 2ALE between the native outer repeat and the wobble-mutagenized inner repeat, and in-frame insertion of exogenous sequences immediately before the 2ALE. Making use of the comparable 3′-duplication approach remains an attractive option for further testing, but has so far been less extensively evaluated.

The extent of genetic stability of the modified rMRVs described here is a matter of substantial importance for considering the potential use of such viruses as transduction vectors in different practical settings. In the current study, we gauged genetic stability as follows: After each plaque-recovered rMRV was subjected to a second round of plaque isolation in L929 cells, we

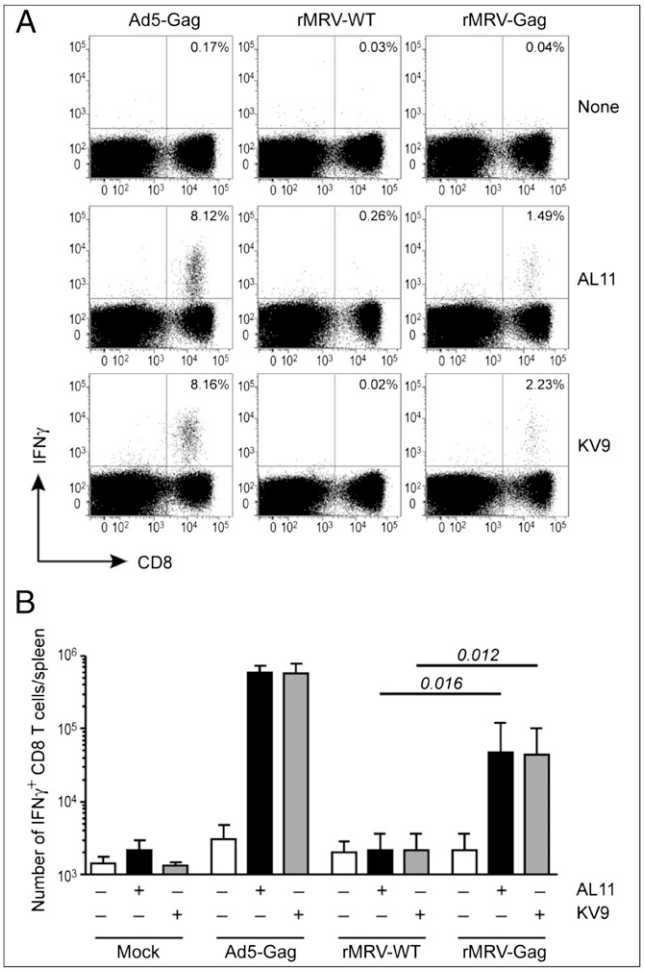

Fig. 4. Immunogenicity of SIVmac239 Gag polypeptide expressed by rMRV in mice. (*A*) Representative flow cytometry plots of splenocytes collected from C57BL/6 mice immunized with an adenovirus 5 vector expressing SIVmac239-Gag (Ad5-Gag) (1×10^9 pfu of purified virions), rMRV WT (1×10^7 pfu of purified virions), or rMRV L1/*gag*900w/2A/5′66w+M1/3′153 (rMRV-Gag) (1×10^7 pfu of purified virions). After collection, the splenocytes were restimulated with no peptide, AL11 peptide, or KV9 peptide, as indicated, followed by staining for surface CD8 (*x* axis) and intracellular IFNγ (*y* axis). (*B*) T-cell responses in immunized mice were quantitated using splenocyte recoveries and percentages of $IFN\gamma^+CD8^+$ T cells after stimulation with no peptide (white bars), AL11 peptide (black bars), or KV9 peptide (gray bars). Error bars, SD from the mean (mock: $n = 2$; Ad5-Gag: $n = 4$; rMRV-WT: $n = 6$; rMRV-Gag: $n = 6$). Significance was determined by one-way unpaired *t*-test, and *P* values are shown for rMRV-Gag relative to rMRV-WT.

additionally subjected each to at least three serial passages in L929 cells, at which point the continued presence of the engineered modifications to MRV genome segment S3, M1, or L1 was confirmed by RT-PCR-based sequencing (*Materials and Methods*). Moreover, dsRNA gels, as shown for certain of the rMRVs in Figs. 2 and 3 and Fig. S1, corroborated that each modified segment exhibited its distinctively slowed electrophoretic mobility in the third-passage samples. Thus, we can reasonably conclude that the modified rMRVs are genetically stable through at least three rounds of passage in L929 cells. Genetic stability in animals has yet to be addressed.

Relating to the question of genetic stability is the issue of how well the modified rMRVs grow relative to WT viruses. Because our studies to date have been milestone-driven to demonstrate the use of rMRVs for eliciting anti-Gag T-cell responses in animals, we have performed relatively few experiments to carefully compare their growth characteristics. The experiment in Fig. 2*C* provides one example suggesting comparable growth of rMRV M1/3′153/2A to rMRV WT in L929 cells. Otherwise, our evidence that the growth of the modified rMRVs is similar to that of rMRV WT is qualitative or semiquantitative, including similar recovery efficiencies from the plasmid cotransfections (10^4–10^5 pfu/mL), similar plaque sizes, similar yields of dsRNA at the passage-three level, similar titers at the passage-two level (10^7–10^8 pfu/mL) when determined, and similar yields and particle/pfu ratios of purified virions obtained and analyzed for the mouse immunization experiments (*Materials and Methods*).

Table 3. Introducing shorter 5′-PARTT regions for recovery into rMRVs

5′-PARTT region length, nt*	rMRV recovery?
201	YES
159	YES
117	YES
96	YES
81	YES
66	YES
51	YES
48	YES
45	YES
42	NO
36	NO
21	NO

*This region comprises the 5′ UTR of S3 plus the outer ORF-region repeat. The length of this region was progressively shortened from a length of 201 nt by deleting nt from its inner (3′ plus strand) end, to yield the region lengths shown in this column. The basal construct for this experiment, containing the 201-nt 5′-PARTT region, was pS3/*gag*27/2A/5′174w.

rMRV Vectors for Expressing Exogenous Polypeptides. The maximum length of 306 aa for the exogenous polypeptides expressed in this study is sufficient for many purposes, but an ability to express even longer polypeptides, including whole proteins such as fluorescent or enzymatic reporters, would be desirable. Although we show that all five of the termini tested (5′ terminus of S3, 5′ and 3′ termini of M1, and 5′ and 3′ termini of L1) are compatible with duplications, an ability to extend to other of the 15 untested termini would also be desirable. Of concern regarding expression from the other segments, however, is how many of the respectively encoded MRV proteins can tolerate the 2ALE-based short extension to their N or C terminus. The myristoylated N terminus of μ1 (34), for example, likely precludes use of the 2ALE at the 5′ end of segment M2. In addition, whether the 2ALE functions with the expected high efficiency (24) in all such settings in rMRVs remains an open question.

The level of exogenous polypeptide expression that can be achieved is another important topic. One way to increase expression may be to apply the strategy to MRV segments whose protein products are translated in largest amounts during infection. The S3 segment studied here is a reasonable choice, according to this criterion, although the M1 and L1 segments are not, as their protein products are produced in below-average amounts among the MRV proteins (35). Thus, in future animal studies, expression of a large portion of Gag from an MRV segment other than L1, which was used for the experiment in Fig. 4, would be expected to increase in vivo expression levels and subsequent Gag-specific responses. Another way to increase expression may be to insert the same exogenous sequences in more than one MRV segment, so that the polypeptide is translated from more than one species of mRNA. However, for certain other uses of the rMRV vectors, maximizing the amount of exogenous polypeptide expression might not be the goal; rather,

titrating expression over a desired range. In that case, being able to express the exogenous polypeptide from several different MRV segments may be helpful, with each segment providing its own unique level of expression (35), as likely determined in part by its terminal PARTT signals.

In addition to the question of expression level, the question of which exogenous polypeptide or polypeptides to express is, of course, crucial, and dictated by the desired application. In this study, we considered one potential use to be in expression of exogenous immunogens, exemplified by SIVmac239 Gag. In the current strategy, the exogenous polypeptide is expressed within rMRV-infected cells, but not subsequently displayed on released virions, as the 2ALE separates the exogenous polypeptide from the MRV protein. Thus, as currently designed, the rMRV vectors would seem to have greater potential for eliciting cellular rather than humoral responses to the exogenous polypeptide, although testing for humoral responses in future experiments would certainly be important to do. Utility of autonomously propagating rMRVs that express reporter proteins is also evident, such as for tracking their spread and tropism in animal models (36). Expression of an exogenous protein to enhance the potential activity of rMRVs as oncolytic agents might also be worthwhile to explore.

rMRVs as Potential Mucosal Vaccine Vectors. We began these efforts to generate rMRVs to express exogenous polypeptides as part of a consortium for developing unique types of potential T-cell-based vaccines targeting HIV-1. As the intestinal subepithelium including Peyer's patches is a major reservoir for HIV-1 amplification and persistence, effective defenses against it may require vaccines targeting the intestinal subepithelium to induce strong CD8 memory T-cell responses in those key mucosal sites (37–39). The intestinal tract is also an important natural route of MRV entry and infection (2). In the gut, MRV induces B-cell responses in Peyer's patches, as well as CD8 T-cell responses in both Peyer's patches and other regions of the subepithelium (40–42). MRV is thus an effective gut mucosal immunogen, eliciting both humoral and cellular responses. Other factors suggesting the potential use of rMRVs as a vaccine platform include the usual mildness of MRV infections of humans and the absence of MRV genome integration into host DNA, given its RNA-only replication scheme. Unfortunately, however, widespread preexisting immunity to MRVs in people (43, 44) is at least one serious problem that would need to be addressed and overcome if rMRV vectors are to be seriously considered as a vaccine platform for targeting HIV-1 or other infectious agents.

Engineering Related dsRNA Viruses as Expression Vectors. MRVs are members of the genus *Orthoreovirus* in family *Reoviridae*, which encompasses 14 other approved genera at this time (1), including the genus *Rotavirus*. The many different viruses in this family infect humans and other vertebrates, as well as arthropods, plants, fungi, and protists. All have between 9 and 12 linear genome segments, and the organization of the genomic plus strands in each virus is very similar to that in MRV (Fig. 1*A*), with one or more ORFs predominating in length and being flanked by much smaller 5′- and 3′-terminal UTRs. Importantly, recent work on rotaviruses has provided strong evidence that 3′-terminal duplications related to ones described here for MRV may be useful for improving on other available systems for rotavirus reverse genetics (45, 46), and by extension, from results described here, for similarly engineering rotavirus vectors for exogenous polypeptide expression. Indeed, the occurrence of such naturally occurring duplications has been known for many years not only for rotaviruses (47, 48) but also for members of genera *Orbivirus*, *Mycoreovirus*, and *Phytoreovirus* (48, 49). Thus, for diverse members of the family *Reoviridae*, duplication and expression strategies similar to ones described here may be useful for developing them as vectors. Another notable recent development in the orbivirus field has been the engineering of an autonomously propagating Bluetongue virus that expresses the fluorescent protein mCherry in fusion with viral protein NS3 (36). This accomplishment nicely illustrates that vector development for any of these viruses including MRV may, in particular circumstances, also use well-chosen sites for exogenous inserts independent of the terminal-duplication strategy described here.

Using the Vector Strategy to Study RNA Capacity and PARTT Activities of MRV. The largest increase in MRV genome size shown in this study is that in L1/*gag*918w/2A/5′207w/ 3′168+M1/3′153, which carries both L1 and M1 insertions (Table 3 and Figs. 2 and 3), for an overall increase of 1,500 bp. The native MRV genome approximates 23,500 bp, so 1,500 bp more represents an increase of >6%.

What is the length of such additional dsRNA sequences that rMRVs can ever accommodate? The MRV inner capsid is formed by 60 dimers of protein λ1 arranged on a T = 1 icosahedral lattice (4). The capsid therefore encloses a central cavity of delimited dimensions, into which the 10-genome segments are packed in locally parallel, liquid crystalline arrays (3, 4). A previous estimate suggests the cavity volume is 84–85% filled by the dsRNA segments and intruding transcriptase complexes in WT MRV (50), further suggesting that an increase in genome size of ∼18% (∼4,300 bp) might be possible to accommodate. The concentration of genomic dsRNA inside the inner capsid of native MRV virions has furthermore been calculated to exceed 400 mg/mL (32), which seems quite high, although many bacteriophages have concentrations of dsDNA near 500 mg/mL (51). In MRVs, unlike these bacteriophages, however, the packaged dsRNA segments must be used as templates for reiterative transcription by the RNA-dependent RNA polymerase molecules within the confines of the inner capsid (4), a process that we have shown to be inhibited by increased intracapsid viscosity (32). Thus, a somewhat lower tolerance for increasing the genome size of MRV, somewhere between the currently observed 1,500-bp increase in L1/*gag*918w/2A/5′207w/3′168+M1/3′153 and the estimated 4,300 bp in extra capacity of the central cavity, seems likely to us. The strategy shown here seems well suited for defining this maximum tolerance. In the case of rotaviruses, an increase in genome size of up to 10% (∼1,800 bp) has so far been observed as a consequence of naturally occurring rearrangements in the genome segments (52).

As illustrated in Table 3, the strategy shown here may also be useful for mapping the minimal PARTT regions at many of the 20 different MRV segment termini. The result for the 5′-PARTT region of S3 differs from previous reports for other MRV segments in being somewhat smaller, at 45 nt, although still extending beyond the 27-nt 5′ UTR of S3 to overlap the essential σNS ORF by 18 nt. The smallest PARTT region previously defined is that at the 5′ end of S2, 96 nt, which extends beyond the 18-bp 5′ UTR to overlap the essential σ2 ORF by 78 nt (13). Such differences between segments seem reasonable to expect and may relate to segment-specific variations in the PARTT activities. To understand these activities, including how the 10 different RNAs are assorted for packaging into each infectious virion, it is therefore important to define the minimal PARTT region at each of the segment termini. In addition, by separating the PARTT and ORF sequences of MRV segments, the strategy shown here may help to pinpoint the PARTT signals by allowing single-nt mutations throughout the PARTT regions in the absence of aa-level effects. Moreover, testing two-way or higher combinations of modified constructs for recovery of rMRVs with two or more modified segments in each might provide a way to identify interactions between the PARTT signals from different segments, which might be important for packaging or assortment.

Materials and Methods

Cells and Viruses. Spinner-adapted murine L929 cells were maintained in Joklik's modified Eagle's MEM (Irvine) supplemented with 2% (vol/vol) fetal and 2% (vol/vol) calf bovine sera (HyClone), 2 mM L-glutamine (Mediatech), 100 U/mL penicillin, and 100 μg/mL streptomycin (Irvine). All rMRVs described in *Results* were grown in L929 cell monolayers to yield cell-lysate stocks, and in some cases, their virions were purified from L929 spinner cultures by Freon extraction and CsCl-gradient centrifugation, as previously described (11). Cell lysate stocks were stored at 4°C, and purified virions were stored at 4°C in virion buffer (150 mM NaCl, 10 mM $MgCl_2$, 10 mM Tris at pH 7.5). MRV virion concentrations (particles/mL) were determined by A_{260} (10). Plaque assays for determining infectious titers (pfu/mL) of the cell lysate stocks and purified virions were performed in L929 cells according to the chymotrypsin overlay protocol (53), with the modification that agar was reduced to 0.5% (vol/vol) to allow earlier plaque visualization.

Modified MRV-Segment Constructs. The pS3/WT, pM1/WT, and pL1/WT plasmids of MRV-T3D (15) (GenBank accession nos. EF494443, EF494438, and EF494435, respectively, for the MRV gene components) were the ones modified in this study. To create tandem duplications, the targeted MRV sequences in these plasmids were amplified in two separate PCR reactions. The fragments were then joined together in a third PCR and inserted into the original MRV-segment plasmid by blunt-end ligation. The duplications ranged from 21 to 207 nt long for different constructs, as indicated elsewhere in the text, figures, and tables.

Exogenous insertions (2ALE and *gag*) were introduced into modified plasmids with PCR primers that contained the desired sequences in their 5′ halves, whereas the 3′ halves were complementary to MRV sequences immediately adjacent to the insertion site. After PCR amplification, the linear copy of the whole plasmid was obtained, now containing the desired insertions at its termini. After removing parental (template) plasmid by DpnI treatment, 5′-phosphorylation and ligation were performed to restore plasmid circularity. For each different construct, 2–5 bacterial colonies were isolated and used to purify, sequence confirm, and separately maintain 2–5 plasmid preparations for subsequent rMRV recovery efforts. The 2ALE insert was 54 nt long in each construct, whereas the *gag* inserts ranged from 27 to 918 nt long for different constructs, as indicated elsewhere in the text, figures, and tables.

Wobble mutations were introduced by a modified QuikChange protocol (Stratagene). The modifications involved use of 30–35 PCR cycles (instead of manufacturer's 12–18 cycles), 72°C elongation (instead of manufacturer's 68°C), and non–manufacturer-supplied buffer, dNTPs, and polymerase (iProof High-Fidelity DNA polymerase; Bio-Rad).

MRV Reverse Genetics. All rMRV recovery experiments were performed using the original plasmid-based protocol of Kobayashi et al. (15), with minor modifications. Plasmids encoding the 10-genome segments of MRV-T3D were kindly provided by T. S. Dermody (Vanderbilt University School of Medicine, Nashville, TN). Attenuated vaccinia virus rDIs-T7 (54) was also provided by T. S. Dermody with permission from T. Miyamura. Our usual yield from cotransfection of the 10 plasmids was in the range of 10^4–10^5 pfu/mL for both rMRV WT and rMRVs with modified segments, as described in *Results*. Plaques recovered from the plasmid cotransfections were first subjected to a second round of plaque isolation and then serially amplified into first and second blind-passage stocks, the latter of which were quantified by plaque assay for certain experiments. Usual titers of these second-passage stocks were in the range of 10^7–10^8 pfu/mL for the different rMRVs, including rMRV WT. It is important to note that if a particular cotransfection of L929 cell monolayers with the 10 WT or modified MRV plasmids yielded plaques in these experiments, those original plaques were successfully used to yield plaques in the subsequent round and also to be amplified into second-passage stocks. Thus, the limitation to obtaining second-passage stocks of some of the rMRVs as described in the text was at the stage of recovering plaques from the plasmid cotransfections, not from failure to grow at a later step.

Second-passage stocks of the rMRVs were used to infect L929 cell monolayers (i.e., a third rMRV passage) for dsRNA analysis, as described in more detail later. On obtaining the dsRNA-gel results, the same dsRNA preparation was as used for RT-PCR-based sequencing to confirm the presence of the expected, modified genome segment. Briefly, primers were designed to allow RT-PCR amplification of a region (consistently longer than 1 kb) encompassing all modifications in a particular segment. The purified RT-PCR products were then directly sequenced to confirm retention of the expected modifications. The RT reaction was performed with SuperScript III (Invitrogen) according to manufacturer's instructions, except that annealing was done with slow cooling from 100°C to room temperature. The PCR was performed with either Taq polymerase (Invitrogen) or iProof High-Fidelity DNA Polymerase (Bio-Rad). Notably, for each modified construct, we used the 2–5 sequence-confirmed plasmid preparations described in the preceding section in separate cotransfections of L929 cell monolayers, from which rMRV plaques were then separately isolated and passaged and again sequence confirmed. In addition, for modified constructs that did not yield plaques from cotransfections, this was consistently found for all 2–5 of the respective plasmid preparations.

Viral dsRNA. L929 monolayers in 6-well plates (~2×10^6 cells/well) were infected with MRV or rMRV at ~10 pfu/cell. After 1 h adsorption at room temperature, the inoculum was removed, cells were washed with PBS, and fresh medium was added. Cells were then incubated at 37°C for 48–60 h, when the medium was aspirated and cells were lysed with 1 mL TRIzol reagent (Invitrogen). RNA was extracted according to the manufacturer's instructions and resuspended in 20 μL of 1 mM EDTA. Seven microliters of extracted dsRNA from each well were loaded onto an SDS/PAGE gel, and dsRNA species were separated by electrophoresis followed by ethidium bromide staining, as described (55), with minor modifications.

In vitro Transcription and Translation. RNA was synthesized in vitro from each respective plasmid (1 μg plasmid/50 μL reaction mix) by using T7 RNA polymerase (1 U/μL; Promega) in the following conditions: 100 mM Hepes at pH 8.1, 20 mM $MgCl_2$, 5 mM of each NTP (GE Healthcare), and 0.5 mM EDTA for 3 h at 37°C. After transcription, RNA was deproteinized by phenol/chloroform extraction, unincorporated NTPs were removed by gel filtration on Microspin G-25 columns (Amersham), and RNA was ethanol-precipitated. The purified RNA was then subjected to in vitro translation in rabbit reticulocyte lysate (Ambion) in the presence of [^{35}S]Met, according to the manufacturer's instructions. Translation products were separated by SDS/PAGE and visualized by phosphorimaging on a Typhoon 9400 Variable Mode Imager with ImageQuant TL software (GE Healthcare). For the experiment in Fig. 2*E*, the original TaV 2ALE insert was mutated to GAGGGCAGGGGCAGCCTGCTGACCTGGGCGACGTGGAGGAGAACCCCGGCCCC, with an underline bracketing the site of the 1-nt (C) deletion.

RNA Folding Predictions. Although folding predictions can be unreliable, we used them as a general guide for trying to reduce RNA structure in the insert-encompassing transcripts. Predicted RNA secondary structures of the *gag* inserts were determined by using NUPACK with default settings as available at http://nupack.org/partition/new (56). On the basis of the folding of each insert, mutations were designed to disrupt predicted base pairs while maintaining the original, encoded protein sequence. After the first round of such mutations, the predicted RNA secondary structure was determined again to check whether any new strongly predicted structures had been unmasked or newly generated. If so, then additional mutations were designed until the desired reduction in predicted structure was achieved.

T-Cell Responses in Immunized Mice. All mice were handled at the Fred Hutchinson Cancer Research Center (FHCRC, Seattle) according to the protocols approved by the University of Washington and FHCRC Institutional Animal Care and Use Committees. Female 6- to 8-wk-old C57BL/6 mice were intramuscularly immunized with PBS (mock); 1×10^5, 1×10^6, or 1×10^7 pfu of negative control rMRV WT; or the same respective doses of L1/*gag*900w/2A/5′66w+M1/3′153. As a positive control, mice were immunized with 1×10^9 pfu of recombinant Ad5 vector expressing SIVmac239-Gag, kindly provided by C. L. Parks, International AIDS Vaccine Initiative, New York (33). The Ad5-Gag dose was chosen based on previous experience (33), whereas lower doses of rMRVs were used in an effort to ensure mouse health throughout the experiment. All recombinant viruses were used as purified virions. In the case of rMRVs WT and L1/*gag*900w/2A/5′66w+M1/3′153, total yields from the purifications and particle/pfu ratios of the purified virions (~1,000) were similar, and the presence of the expected, modified L1 segment in the latter was confirmed again by sequencing from genomic dsRNA released from the purified virions. At 7 d postimmunization, mice were killed, and splenocytes were restimulated for 5 h with no peptide or with the previously defined AL11- or KV9-epitope-containing peptides (30) in the presence of brefeldin A. CD8 T-cell responses were detected by surface labeling with anti-CD8a-PE antibody (clone 53–6.7, BD Biosciences) in FACS buffer [PBS, 1% (wt/vol) BSA, 0.1% (wt/vol) NaN_3], followed by permeabilization and intracellular staining with anti-IFNγ-FITC antibody (clone XMG1.2, BD Biosciences). Samples were then fixed in 2% (vol/vol) paraformaldehyde and immediately analyzed on a FACSCanto II flow cytometer (BD Biosciences).

ACKNOWLEDGMENTS. We thank E. Freimont and S. Boulant for technical assistance and advice; T. Dermody for the kind gifts of MRV-T3D plasmids and vaccinia virus rDIs-T7; C. Parks and the Collaboration for AIDS Discovery team at the International AIDS Vaccine Initiative for kind gifts of SIVmac239 plasmid and Ad5-Gag virions; and D. Knipe, C. Parks, and S. Whelan for comments on the manuscript. We also thank members of the International AIDS Vaccine Initiative Scientific Advisory Committee and members of the International AIDS Vaccine Initiative Vector Design Consortium for helpful discussions and encouragement over the course of these studies. We are especially grateful to T. Zamb, C. Parks, R. Boyle, B. Rasmussen, and B. Turk for their patience and kind support. This study was supported by Collaboration for AIDS Discovery grants from the Bill and Melinda Gates Foundation to the Zamb/Parks Vector Design Consortium (2006–2011) and the Greenberg Mouse Immunology Laboratory.

1. Attoui H, et al. (2011) Reoviridae. *Virus Taxonomy: Ninth Report of the International Committee on Taxonomy of Viruses*, eds King AMQ, Adams MJ, Carstens EB, Lefkowitz EJ (Elsevier/Academic, Waltham, MA), pp 541–637.
2. Schiff LA, Nibert ML, Tyler KL (2007) Orthoreoviruses and their replication. *Fields Virology*, eds Knipe DM, Howley PM (Wolters Kluwer Health/Lippincott Williams & Wilkins, Philadelphia), 5th Ed, pp 1853–1915.
3. Dryden KA, et al. (1993) Early steps in reovirus infection are associated with dramatic changes in supramolecular structure and protein conformation: Analysis of virions and subviral particles by cryoelectron microscopy and image reconstruction. *J Cell Biol* 122(5):1023–1041.
4. Reinisch KM, Nibert ML, Harrison SC (2000) Structure of the reovirus core at 3.6 Å resolution. *Nature* 404(6781):960–967.
5. Weiner HL, Drayna D, Averill DR, Jr., Fields BN (1977) Molecular basis of reovirus virulence: Role of the S1 gene. *Proc Natl Acad Sci USA* 74(12):5744–5748.
6. Tyler KL, McPhee DA, Fields BN (1986) Distinct pathways of viral spread in the host determined by reovirus S1 gene segment. *Science* 233(4765):770–774.
7. Shmulevitz M, Marcato P, Lee PWK (2005) Unshackling the links between reovirus oncolysis, Ras signaling, translational control and cancer. *Oncogene* 24(52): 7720–7728.
8. Fields BN (1971) Temperature-sensitive mutants of reovirus type 3 features of genetic recombination. *Virology* 46(1):142–148.
9. Spriggs DR, Fields BN (1982) Attenuated reovirus type 3 strains generated by selection of haemagglutinin antigenic variants. *Nature* 297(5861):68–70.
10. Chandran K, et al. (1999) In vitro recoating of reovirus cores with baculovirus-expressed outer-capsid proteins μ1 and σ3. *J Virol* 73(5):3941–3950.
11. Chandran K, et al. (2001) Complete in vitro assembly of the reovirus outer capsid produces highly infectious particles suitable for genetic studies of the receptor-binding protein. *J Virol* 75(11):5335–5342.
12. Roner MR, Joklik WK (2001) Reovirus reverse genetics: Incorporation of the CAT gene into the reovirus genome. *Proc Natl Acad Sci USA* 98(14):8036–8041.
13. Roner MR, Steele BG (2007) Localizing the reovirus packaging signals using an engineered m1 and s2 ssRNA. *Virology* 358(1):89–97.
14. Roner MR, Steele BG (2007) Features of the mammalian orthoreovirus 3 Dearing l1 single-stranded RNA that direct packaging and serotype restriction. *J Gen Virol* 88(Pt 12):3401–3412.
15. Kobayashi T, et al. (2007) A plasmid-based reverse genetics system for animal double-stranded RNA viruses. *Cell Host Microbe* 1(2):147–157.
16. Kobayashi T, Ooms LS, Ikizler M, Chappell JD, Dermody TS (2010) An improved reverse genetics system for mammalian orthoreoviruses. *Virology* 398(2):194–200.
17. Ooms LS, Kobayashi T, Dermody TS, Chappell JD (2010) A post-entry step in the mammalian orthoreovirus replication cycle is a determinant of cell tropism. *J Biol Chem* 285(53):41604–41613.
18. Ivanovic T, et al. (2011) Recruitment of cellular clathrin to viral factories and disruption of clathrin-dependent trafficking. *Traffic* 12(9):1179–1195.
19. Frierson JM, et al. (2012) Utilization of sialylated glycans as coreceptors enhances the neurovirulence of serotype 3 reovirus. *J Virol* 86(24):13164–13173.
20. van den Wollenberg DJ, et al. (2008) A strategy for genetic modification of the spike-encoding segment of human reovirus T3D for reovirus targeting. *Gene Ther* 15(24): 1567–1578.
21. Brochu-Lafontaine V, Lemay G (2012) Addition of exogenous polypeptides on the mammalian reovirus outer capsid using reverse genetics. *J Virol Methods* 179(2): 342–350.
22. Zou S, Brown EG (1992) Identification of sequence elements containing signals for replication and encapsidation of the reovirus M1 genome segment. *Virology* 186(2): 377–388.
23. Ni Y, Kemp MC (1994) Subgenomic S1 segments are packaged by avian reovirus defective interfering particles having an S1 segment deletion. *Virus Res* 32(3): 329–342.
24. Donnelly ML, et al. (2001) The 'cleavage' activities of foot-and-mouth disease virus 2A site-directed mutants and naturally occurring '2A-like' sequences. *J Gen Virol* 82(Pt 5): 1027–1041.
25. Szymczak AL, et al. (2004) Correction of multi-gene deficiency in vivo using a single 'self-cleaving' 2A peptide-based retroviral vector. *Nat Biotechnol* 22(5):589–594.
26. Pringle FM, et al. (1999) A novel capsid expression strategy for Thosea asigna virus (*Tetraviridae*). *J Gen Virol* 80(Pt 7):1855–1863.
27. Doronina VA, et al. (2008) Site-specific release of nascent chains from ribosomes at a sense codon. *Mol Cell Biol* 28(13):4227–4239.
28. Carvalho J, Arnold MM, Nibert ML (2007) Silencing and complementation of reovirus core protein μ2: Functional correlations with μ2-microtubule association and differences between virus- and plasmid-derived μ2. *Virology* 364(2):301–316.
29. Regier DA, Desrosiers RC (1990) The complete nucleotide sequence of a pathogenic molecular clone of simian immunodeficiency virus. *AIDS Res Hum Retroviruses* 6(11): 1221–1231.
30. Liu J, et al. (2006) Modulation of DNA vaccine-elicited CD8+ T-lymphocyte epitope immunodominance hierarchies. *J Virol* 80(24):11991–11997.
31. Mothé BR, et al. (2002) Dominance of CD8 responses specific for epitopes bound by a single major histocompatibility complex class I molecule during the acute phase of viral infection. *J Virol* 76(2):875–884.
32. Demidenko AA, Lee J, Powers TR, Nibert ML (2011) Effects of viscogens on RNA transcription inside reovirus particles. *J Biol Chem* 286(34):29521–29530.
33. Winstone N, et al. (2011) Enhanced control of pathogenic Simian immunodeficiency virus SIVmac239 replication in macaques immunized with an interleukin-12 plasmid and a DNA prime-viral vector boost vaccine regimen. *J Virol* 85(18):9578–9587.
34. Nibert ML, Schiff LA, Fields BN (1991) Mammalian reoviruses contain a myristoylated structural protein. *J Virol* 65(4):1960–1967.
35. Gaillard RK, Jr., Joklik WK (1985) The relative translation efficiencies of reovirus messenger RNAs. *Virology* 147(2):336–348.
36. Shaw AE, et al. (2012) *Drosophila melanogaster* as a model organism for bluetongue virus replication and tropism. *J Virol* 86(17):9015–9024.
37. Belyakov IM, Ahlers JD (2008) Functional CD8+ CTLs in mucosal sites and HIV infection: Moving forward toward a mucosal AIDS vaccine. *Trends Immunol* 29(11):574–585.
38. Hansen SG, et al. (2011) Profound early control of highly pathogenic SIV by an effector memory T-cell vaccine. *Nature* 473(7348):523–527.
39. McDermott AB, Koup RA (2012) CD8(+) T cells in preventing HIV infection and disease. *AIDS* 26(10):1281–1292.
40. London SD, Rubin DH, Cebra JJ (1987) Gut mucosal immunization with reovirus serotype 1/L stimulates virus-specific cytotoxic T cell precursors as well as IgA memory cells in Peyer's patches. *J Exp Med* 165(3):830–847.
41. London SD, Cebra JJ, Rubin DH (1989) Intraepithelial lymphocytes contain virus-specific, MHC-restricted cytotoxic cell precursors after gut mucosal immunization with reovirus serotype 1/Lang. *Reg Immunol* 2(2):98–102.
42. Chen D, Rubin DH (2001) Mucosal T cell response to reovirus. *Immunol Res* 23(2-3): 229–234.
43. Lerner AM, Cherry JD, Klein JO, Finland M (1962) Infections with reoviruses. *N Engl J Med* 267:947–952.
44. Tai JH, et al. (2005) Prevalence of reovirus-specific antibodies in young children in Nashville, Tennessee. *J Infect Dis* 191(8):1221–1224.
45. Troupin C, et al. (2010) Rearranged genomic RNA segments offer a new approach to the reverse genetics of rotaviruses. *J Virol* 84(13):6711–6719.
46. Troupin C, et al. (2011) Rotavirus rearranged genomic RNA segments are preferentially packaged into viruses despite not conferring selective growth advantage to viruses. *PLoS ONE* 6(5):e20080.
47. Desselberger U (1996) Genome rearrangements of rotaviruses. *Adv Virus Res* 46:69–95.
48. Tanaka T, Eusebio-Cope A, Sun L, Suzuki N (2012) Mycoreovirus genome alterations: Similarities to and differences from rearrangements reported for other reoviruses. *Front Microbiol* 3:186.
49. Anthony SJ, et al. (2011) RNA segment 9 exists as a duplex concatemer in an Australian strain of epizootic haemorrhagic disease virus (EHDV): Genetic analysis and evidence for the presence of concatemers as a normal feature of orbivirus replication. *Virology* 420(2):164–171.
50. Nibert ML (1998) Structure of mammalian orthoreovirus particles. *Curr Top Microbiol Immunol* 233(Pt 1):1–30.
51. Earnshaw WC, Casjens SR (1980) DNA packaging by the double-stranded DNA bacteriophages. *Cell* 21(2):319–331.
52. McIntyre M, et al. (1987) Biophysical characterization of rotavirus particles containing rearranged genomes. *J Gen Virol* 68(Pt 11):2961–2966.
53. Middleton JK, et al. (2002) Thermostability of reovirus disassembly intermediates (ISVPs) correlates with genetic, biochemical, and thermodynamic properties of major surface protein μ1. *J Virol* 76(3):1051–1061.
54. Ishii K, et al. (2002) Structural analysis of vaccinia virus DIs strain: Application as a new replication-deficient viral vector. *Virology* 302(2):433–444.
55. Moody MD, Joklik WK (1989) The function of reovirus proteins during the reovirus multiplication cycle: Analysis using monoreassortants. *Virology* 173(2):437–446.
56. Zadeh JN, et al. (2011) NUPACK: Analysis and design of nucleic acid systems. *J Comput Chem* 32(1):170–173.